

© Copyright 1987 American Meteorological Society (AMS). Permission to use figures, tables, and brief excerpts from this work in scientific and educational works is hereby granted provided that the source is acknowledged. Any use of material in this work that is determined to be “fair use” under Section 107 of the U.S. Copyright Act or that satisfies the conditions specified in Section 108 of the U.S. Copyright Act (17 USC §108, as revised by P.L. 94-553) does not require the AMS’s permission. Republication, systematic reproduction, posting in electronic form on servers, or other uses of this material, except as exempted by the above statement, requires written permission or a license from the AMS. Additional details are provided in the AMS CopyrightPolicy, available on the AMS Web site located at (<http://www.ametsoc.org/AMS>) or from the AMS at 617-227-2425 or [copyright@ametsoc.org](mailto:copyright@ametsoc.org).

Permission to place a copy of this work on this server has been provided by the AMS. The AMS does not guarantee that the copy provided here is an accurate copy of the published work.

Marilyn M. Wolfson and T. Theodore Fujita

Massachusetts Institute of Technology  
Lincoln Laboratory  
Lexington, MA 02173

The University of Chicago  
Department of the Geophysical Sciences  
Chicago, IL 60637

## 1. INTRODUCTION

The FLOWS (FAA-Lincoln Laboratory Operational Weather Studies) Project is developing methods for automatically detecting and warning against aviation weather hazards, such as low-altitude wind shear, in airport terminal areas using NEXRAD-like Doppler weather radars. Currently, the FAA uses the Low Level Wind Shear Alert System (LLWAS), an anemometer array situated within and around an airport terminal area, for real-time detection of wind shear events. Even with the installation of Terminal Doppler Weather Radars (TDWRs) at some airports, the LLWAS systems there could still play an important role in the accurate detection of wind shear events, and at airports without TDWRs, the LLWAS will remain the primary detection system.

The slowing or obstruction of wind by local obstacles is a well known problem to those wishing to make accurate wind speed measurements. Anemometers should always be located where there will be, as nearly as possible, an unobstructed wind flow free from turbulent eddies in all directions. Because of the fairly precise required sensor configuration of the anemometers in an LLWAS system, it can occasionally be difficult or impossible to find sites with good exposure in all directions.

The FLOWS project is interested in the unobstructed wind speed measurements for two main reasons. First, when analyzing a snapshot of the wind field over a mesonet (or LLWAS) for horizontal wind shear and/or for comparison with Doppler radar data, use of the measured, uncorrected winds would reveal spurious patterns of divergence or vorticity that depend little on time but greatly on the prevailing wind direction and that would, in some cases, obscure the true wind shear pattern. Second, when using surface wind measurements to estimate winds aloft that might be encountered by an aircraft on take-off or landing, an appropriate power law can be accurately used if the original surface wind speed

measurements are representative of the unobstructed flow.

## 2. THE STUDY

As part of the FLOWS Project in 1985, Lincoln Laboratory operated a network of 30 automatic weather stations (Wolfson, *et al.*, 1986; Wolfson, 1987) in the vicinity of the Memphis International Airport and also continuously recorded data from the Memphis Airport LLWAS system. The exposure of all 6 LLWAS and 30 mesonet sites was evaluated using anemometer data taken over 197 days from 15 February through 31 August. Our analysis shows unquestionably that substantial differences of up to 50% existed between the stations that were related to the degree of site obstruction (see Fig. 1 and Table 1). While subjective wind field analyses, with the aid of panoramic photographs and topographic maps, could have been used to help correct the problem for individually studied wind events, an accurate automated procedure was desired for potential utilization in an operational system. A time-independent technique for mathematically correcting the measured wind speeds as a function of azimuth at each site, that could be used in real-time in a system such as the LLWAS, is derived. The technique is a more generalized and improved version of that used by Fujita and Wakimoto (1982), referred to hereafter as FW.

## 3. TRANSMISSION FACTORS

First, it is assumed that the measured wind speed,  $V$ , can be expressed as

$$V = U \psi \quad (1)$$

where  $U$  is the unobstructed wind speed at anemometer height and  $\psi$  is the fraction of the unobstructed wind "transmitted" into the wake region behind an obstruction. It is quite easy to imagine the character and pattern of the obstruction wake flow varying with the magnitude of the wind, but here, in Eq. (1), it is implicitly assumed that the measured wind speed is linearly proportional to the unobstructed wind speed. This is an imperfect assumption

\*The work described here was sponsored by the Federal Aviation Administration. The United States Government assumes no liability for its content or use thereof.

that represents only a first approximation to the true relationship.

The spatial scale over which the unobstructed wind varies is assumed to be >400 km, much larger than that of the FLOWS network; thus the value of  $U$  can be considered uniform across the network. However, the speed and direction of the unobstructed wind vary with time, as do the speed and direction of the measured wind. But if the ratio of the measured to the unobstructed wind speed, defined as the transmission factor  $\psi$ , can be related to the specific site obstructions, then in principle any time variations in  $\psi$  would be caused by time variations in the obstructions themselves or by changes in the characteristics of the obstructed wake flow. The wake flow pattern could change, for example, as a function of wind speed and the permeability of the obstructions themselves or because of changes in the stability of the atmospheric boundary layer. Neglecting these possible time variations, Eq. (1) becomes

$$V(s,d) = U(d) \psi(s,d) \quad (2)$$

where  $s$  is the particular weather station site and  $d$  is the measured wind direction. With estimates of  $\psi(s,d)$ , Eq. (2) can be used to find the unobstructed wind speed at any time.

The unobstructed wind speed can be estimated as a function of azimuth, as was done by FW, by assuming it is equal to the highest mean wind speed measured by any of the stations (mesonet and LLWAS) in a given direction over a long-term average. In this case, the average over all 197 days of data was used. The five stations nearest to the center of the airport accounted for most of these measurements; in all they accounted for 337 out of 360 elements, or 94%, of the estimated unobstructed wind array. Panoramic photographs (not shown) reveal that at each of these stations, in the directions where the measured winds were the highest, the airflow was essentially unobstructed. Even without directional considerations, the mean wind speed map (Fig. 1) reveals a significant maximum of 3.0 m/s and higher directly over the airport.

Unrealistic variations are present in the unobstructed wind speed array,  $U(d)$ , when the components are selected every  $1^\circ$  in azimuth as they were here. Following FW, a weighting function was used to smooth azimuthal variations:

$$G = 1 + \cos(n\lambda) \quad -180^\circ < n\lambda < +180^\circ. \quad (3)$$

The  $30^\circ$  width was found to eliminate unwanted variations while not oversmoothing the data. The unobstructed wind speed  $U(d)$  used for the calculation of the transmission factors was thus defined as

$$U_{30} = \sum \bar{v} G(30^\circ) / \sum G(30^\circ) \quad (4)$$

where  $\bar{v}$  is the highest time averaged wind speed of all the stations in a given direction and  $G(30^\circ)$  is the weighting function in Eq. (3) applied with a  $30^\circ$  width.

The time averaged wind speed as a function of wind direction for each station,  $V(s,d)$ , was also smoothed in azimuth and, after experimenting with weighting functions of varying widths up to  $30^\circ$ , a  $16^\circ$  wide function was selected. Therefore,

$$V_{16} = \sum V G(16^\circ) / \sum G(16^\circ). \quad (5)$$

The transmission factors at each station are defined as:

$$\psi(s,d)_{16} = V_{16}(s,d) / U_{30}(d). \quad (6)$$

The transmission,  $\psi_{16}$ , is essentially a measured quantity; time series of surface wind measurements from a network of anemometers are all that are needed for its calculation at a particular site.

#### 4. SCALE-DEPENDENT TRANSMISSION FACTORS

It is clear from Table 1 and Fig. 1 that some correlation exists between the visible obstructions above the horizon at a particular site and the mean wind speed measured there. Obstructions on this local, visible scale (40 m - 4 km, microscale) might well account for most of the observed wind speed transmission at a station. The effects of the visible microscale obstructions on measured wind speeds are estimated by first determining the empirical relationship between them, and then determining how much of the measured transmission at each station can be predicted based on this relationship.

The local obstructions at each site were characterized by the elevation angles above the horizon of visible objects in a panoramic ( $360^\circ$ ) photograph taken near anemometer level. The obstruction angles were manually estimated to the nearest degree for each azimuth. These values were also smoothed in azimuth with a  $16^\circ$  weighting function:

$$\theta(s,d) = \sum \theta G(16^\circ) / \sum G(16^\circ). \quad (7)$$

The panoramic photograph, and the corresponding smoothed obstruction angle curve and transmission factor curve are shown for station No. 23 in Fig. 2. The mean obstruction angle and mean transmission factor for each site are given in Table 1.

The values of  $\theta_{16}$  and  $\psi_{16}$  for each station, for every degree of azimuth, are plotted against each other in Fig. 3. Since many measurements exist at low obstruction angles, the mean value of the transmission factors for every  $0.1^\circ$  in elevation angle was computed and the results plotted in Fig. 4. The variance of the points increases with increasing elevation angle because fewer of these higher angles were observed. The best exponential curve, fit using all of the data points (not just the mean at every  $0.1^\circ$ ), is also plotted in Fig. 4. It represents the

functional relationship between  $\psi$  and  $\theta$  for the FLOWS network:

$$\psi = 0.42 + 0.35 \exp[-0.18 \theta] \quad (8)$$

where  $\theta$  is in degrees.

Notice that when  $\theta=0^\circ$ ,  $\psi$  does not equal 1 but is offset at 0.77. Yet, in an otherwise uniform environment, the transmission factor should increase to 1 an infinite distance downwind of the obstruction where the visible obstruction angle (actually the tangent of the angle\*) approaches  $0^\circ$ .

Following FW, it is assumed that

$$\psi = \psi_e \psi_i \quad (9)$$

where  $\psi_e$  accounts for large-scale (4 km - 400 km, mesoscale) obstruction effects and  $\psi_i$ , for microscale obstruction effects. It is assumed that  $\psi_i = 1$  when  $\theta = 0^\circ$ ;  $\psi_e$  then is equal to the remaining value of  $\psi$  when  $\theta = 0^\circ$ , that is:

$$\psi = 0.77 \psi_i \quad (10)$$

Combining Eqs. (8) and (10), the relationship between the visible microscale obstructions and wind speed transmissions is found to be:

$$\psi = .545 + .455 \exp[-0.18 \theta]. \quad (11)$$

Notice that, no matter how large the obstruction angle  $\theta$ ,  $\psi_i$  is never less than 0.545 and  $\psi$  never less than 0.42, representing correction factors (the reciprocals) of 1.83 and 2.38, respectively, to the measured wind speeds. A similar equation derived by FW had no additive term but had an exponential decay constant of  $-0.0948$ , roughly half of that observed here (Fig. 4, curve B); at  $\theta=25^\circ$  the total microscale transmission would be only 0.09, implying a correction factor of over 10 to the measured wind speed. The data collected in the FLOWS experiment reveal that as the obstruction angles increase above  $\sim 10^\circ$  there is little further change in observed transmission.

It is perhaps useful to reconcile the approach used by FW with that used here. FW assumed that

$$\psi_i = \exp[-k\theta] \quad (12)$$

and 
$$\psi = \psi_e \psi_i = C \exp[-k\theta] \quad (13)$$

where  $C$  is a constant for all obstruction angles (but varies in azimuth at each site).  $\psi_i$  was first derived by finding the value of  $k$  which caused the correlation between  $\theta$  and

$$\psi/\psi_i = \psi \exp[+k\theta] \quad (14)$$

to approach zero. But this is just the equation for  $\psi_e$ ! The exponential constant,  $k$ , is just the value that explains all of the variation of  $\psi$  with  $\theta$ , and allows  $C$  in Eq. (13) to be fully independent of  $\theta$ , that is, to be a constant. Furthermore, successively testing values of  $k$  that minimize the correlation at each site between  $\theta$  and  $\psi_e$  as given in Eq. (14) or, equivalently, that maximize the negative correlation between  $\psi$  and  $\theta$ , simply amounts to finding approximate solutions that minimize the error in a regression problem that, in this case, can be solved exactly. Taking the logarithm of Eq. (13),

$$\ln \psi = \ln C - k\theta \quad (15)$$

or 
$$Y = A + BX \quad (16)$$

where  $A=\ln C$  and  $B=-k$  are constants. With this linear relationship, the method of least squares provides a simple formula for the "best" estimates of  $A$  and  $B$ . The correlation is a measure of the relationship between two variables and so is  $B$  in Eq. (16). In FW, the value of  $k$  that minimized the correlation between  $\psi_e$  and  $\theta$  was found for each station and these values of  $k$  were averaged together, each weighted with the correlation between  $\psi$  and  $\theta$  at that site, to derive a value of  $k$  for the network. This is equivalent to finding the best fit line ( $Y=A+BX$ ) at each station, and then finding the mean value of the slopes,  $B$ , for the network by weighting each value of  $B$  with itself, multiplied by the ratio of the variance in  $X$  ( $\theta$ ) to the variance in  $Y$  ( $\ln \psi$ ) at that station. Perhaps a better approach would have been to find the "network"  $k$  directly by using the data from all of the stations at once in solving the regression problem.

This latter approach was used here, except the curve being fit was of the form

$$\psi = A + C \exp[-k\theta]. \quad (17)$$

An iterative procedure was used to find the values of  $A$ ,  $C$ , and  $k$  which minimized the sum of the squares of the errors between the observed values of  $\psi$  at all of the stations and those estimated with Eq. (17).

Once the microscale transmission factors,  $\psi_i$ , have been calculated from the obstruction angles at each station according to Eq. (11), the mesoscale transmission factors,  $\psi_e$ , can be calculated from Eq. (9). The  $\psi_e$  are independent of  $\theta$ , and have a mean of 0.77, but they are still functions of azimuth, or wind direction ( $d$ ), at each weather station site. Plots of these values (Wolfson, *et al.*, 1986) show such a striking consistency from one station to the next, and in the pattern set up over the network as the wind blows from a given direction, that it discourages any conclusion that these numbers are simply randomly distributed. Apart from any effects of the visible obstructions at these sites, which were removed in the microscale transmission factors, clearly significant effects of what is

\*Most studies have shown that the transmission factor decreases exponentially as the ratio of obstruction height to the downwind distance ( $\tan \theta$ ) increases. The use of  $\theta$  as an approximation to  $\tan \theta$  is valid for these purposes up to angles of  $25^\circ$  where the error is roughly 6%. The largest observed obstruction angle in the FLOWS network was  $24^\circ$ .

assumed to be the larger scale "obstruction horizon" are evident in the data. The largest contribution to  $\psi_e$  is probably from features just beyond those visible, such as topographical variations on the 2-20 km scale, and from features such as the city of Memphis (20-40 km scale).

## 5. TIME-DEPENDENT TRANSMISSION FACTORS

The possibility that the observed transmission factors are time-dependent at a given site has also been explored. Since the observed obstructions, namely trees and vegetation for the FLOWS Project in Memphis, change in size, density, and character with the changing seasons, it is plausible that the transmission factors might also change. It was found that while a very slight bit of accuracy might be gained by using seasonal transmission factors, this procedure was definitely not necessary. Certainly if one chooses not to add the complication of seasonal transmission factors, then one would surely not want to consider an even finer time scale such as monthly. But the correlations between the monthly and the total transmission factors can help answer the practical question of how much data should be used to accurately estimate the total transmission factors. It was found that the transmission factors were quite similar from month to month, suggesting that one month's data (from sensors with high data quality) would allow an accurate estimate of the time-independent transmission factors, although the more data used in making the estimate, the better.

## 6. SUMMARY

It appears that the effects of obstructions of different scales on winds at a particular site can be quantified. A strong, negative correlation was found between the observed transmission factors and the measured obstruction angles. The functional relationship between them was modelled as a decaying exponential plus a constant. It was found that the first 8° of obstruction have the greatest blockage effects; the contributions of higher obstructions become proportionally less great. Even a 2° or 3° high isolated clump of trees can have a measurable, pronounced effect on the measured wind speeds from that direction. The ratio of the observed transmission,  $\psi$ , to the calculated microscale transmission,  $\psi_i$ , was taken to represent the transmission through obstructions on a scale larger than visible, the mesoscale. It was found that contributions from 2-40 km spatial scales were represented and discernable, with the smaller scales having the greatest impact on the measured winds.

In recommending a wind correction procedure, the final use of the data must be considered. The variations in the wind speed measurements across the weather station network are quite real; they are partly due to surface irregularities and obstructions and partly due to actual patterns of divergence and vorticity in the unobstructed flow. (Of course, part of the variation could always be due to

individual sensor characteristics.) Any time one wishes to analyze the unobstructed flow, as is the case when the measurements are to be compared with Doppler radar data, wind corrections should be applied. But, is it more appropriate to correct wind patterns with spatial variations on small scales (<4 km) for obstruction effects on only that scale, or should all winds be corrected for both visible microscale and larger mesoscale obstructions? Since the FLOWS project is concerned with identifying and understanding microbursts, with horizontal scales by definition less than 4 km, it is recommended that visible correction factors *only* be used. If gust fronts or larger scale wind shear phenomena were of primary interest, then the measured winds should be corrected for both visible and larger scale obstructions.

Another possibility not explored in this study is that the wind correction factors are a nonlinear function of the measured wind speed. This is quite probable considering the complexity of wake flow dynamics. Intuitively, it must be wrong to correct measured wind speeds of 25-30 m/s by the same factor (in some cases more than a factor of 2) used to correct wind speeds of 5-10 m/s, no matter what the obstruction. The factors derived here are actually most appropriate for speeds near the observed mean of 2.67 m/s. Application of the calculated wind speed correction factors to a few selected microburst events did reveal a persistent overestimation of the unobstructed flow. Finding empirically the transmission factors (wind speed correction factors) as a function of wind direction, observed obstruction angle, and measured wind speed will be an important extension for future work.

## ACKNOWLEDGEMENTS

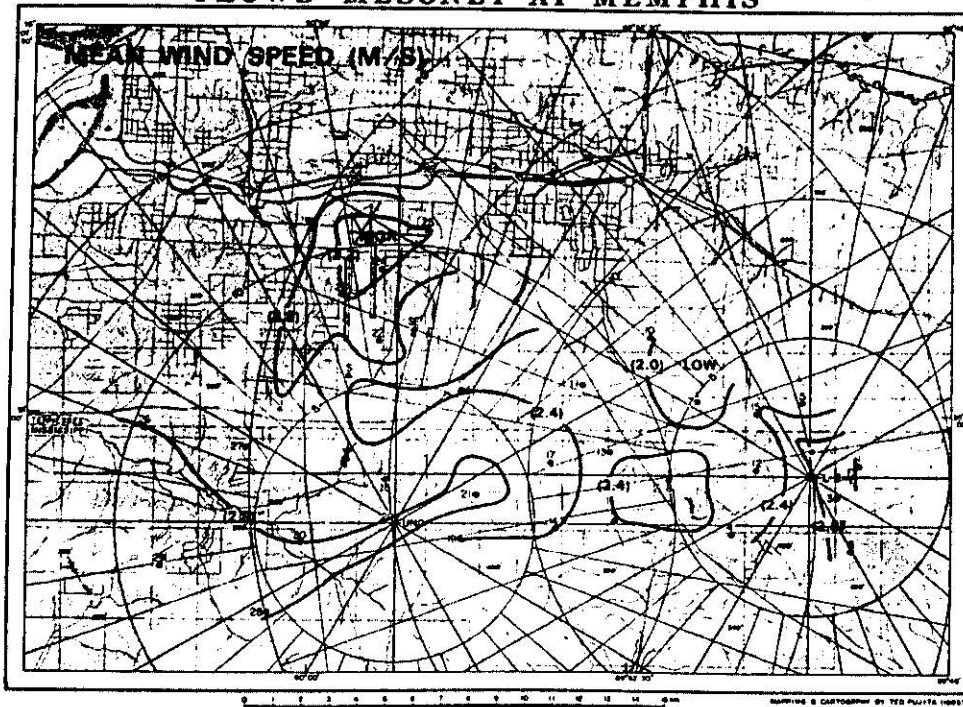
We thank John DiStefano for his help in completing the analyses presented here, and Barbara Forman for her programming assistance. We gratefully acknowledge the work of Dr. Roger Wakimoto in performing the "FW" study, of which the current study is a simple extension. We also thank Charles Curtiss for doing a great job of keeping the FLOWS mesonet up and running, Bill Drury for implementing the LLWAS recording system, and Dr. Jim Evans for his consistent support.

## REFERENCES

- Fujita, T.T. and R.M. Wakimoto, 1982: Effects of micro- and meso-scale obstructions on PAM winds obtained during Project NIMROD. *J. Appl. Meteor.*, 21, 840-858.
- Wolfson, M.M., 1987: The FLOWS automatic weather station network. *Preprints, 6th Symposium on Meteorological Observations and Instrumentation*, New Orleans, Amer. Meteor. Soc. (this Preprint volume).
- Wolfson, M.M., J.T. DiStefano, and B.E. Forman, 1986: The FLOWS automatic weather station network in operation. *Project Report ATC-134*, MIT Lincoln Laboratory, FAA Report No. DOT-FAA-PM-85/27, 284 pp (in preparation).



## FLOWS MESONET AT MEMPHIS



STATION NUMBER	MEAN WIND SPEED	MEAN OBSTRUCTION ANGLE (°)	MEAN TRANSMISSION FACTOR	NUMBER OF WIND MEASUREMENTS
1	3.03	2.1	0.75	253,323
2	3.05	1.0	0.75	249,020
3	2.96	1.4	0.73	254,083
4	2.29	3.7	0.56	240,464
5	2.18	4.3	0.56	238,576
6	2.85	1.1	0.73	249,018
7	1.83	8.7	0.47	190,602
8	2.79	1.6	0.70	240,603
9	2.43	3.0	0.61	224,126
10	1.99	4.7	0.51	234,554
11	2.31	8.9	0.50	224,298
12	2.03	6.8	0.49	237,109
13	2.33	3.6	0.59	238,168
14	2.42	2.4	0.61	223,306
15	2.44	6.1	0.60	249,188
16	2.41	3.8	0.62	239,755
17	2.46	2.3	0.65	222,126
18	2.34	3.2	0.59	250,485
19	2.43	2.4	0.59	240,849
20	2.86	1.7	0.74	253,509
21	2.96	0.9	0.73	252,343
22	3.13	0.7	0.82	246,738
23	3.24	2.0	0.78	240,049
24	3.23	1.9	0.81	251,085
25	3.23	2.0	0.82	258,999
26	2.83	2.8	0.71	228,298
27	2.67	1.6	0.68	226,115
28	2.77	2.8	0.70	242,522
29	3.01	0.8	0.74	238,826
30	2.84	1.8	0.75	228,791
CF	3.56	0.3	0.88	242,710
N	2.54	0.3	0.63	233,075
E	2.87	0.3	0.73	236,518
SE	2.47	0.1	0.58	231,630
S	2.35	0.4	0.62	238,991
W	2.65	0.3	0.66	233,393
NETWORK MEAN	2.67	2.5	0.67	8,583,245

Figure 1. Mean wind speed averaged over 197 days (15 February – 31 August, 1985) at 6 Memphis LLWAS stations (black triangles) and 30 FLOWS automatic weather stations (black circles). The effects of open terrain near both the Memphis International Airport and the small Olive Branch, MS airport (near FL-2 radar site) can be seen. Values at station No. 7 (1.8 m/s) and LLWAS Center Field (3.6 m/s) differ by a factor of 2.

Table 1. The mean wind speed values averaged over 197 days (15 February – 31 August, 1985), the mean obstruction angles ( $\theta$ ) and mean transmission factors ( $\psi$ ) averaged over 360° azimuth, and the total number of measurements used in computing the mean wind speed values are given for the FLOWS mesonet stations and the FAA LLWAS stations. The location of each of the stations is shown in Fig. 1.

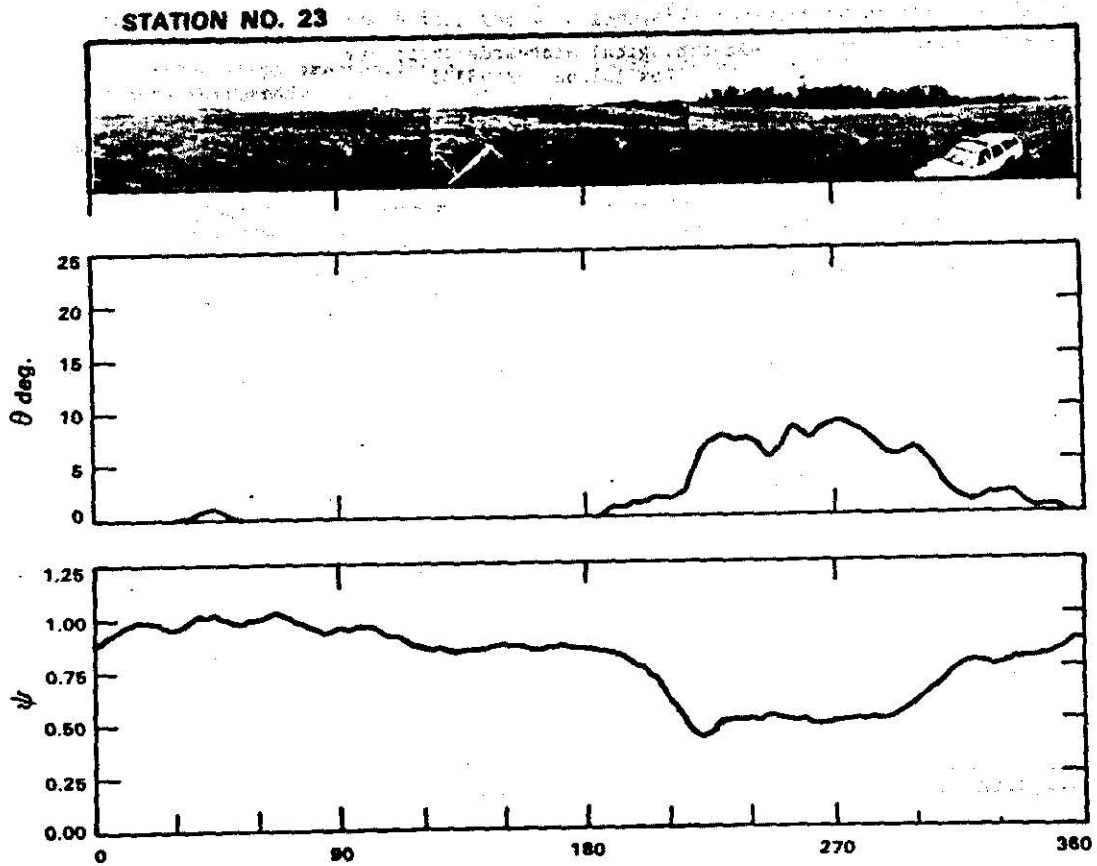


Figure 2. Panoramic photograph, plot of smoothed obstruction angles,  $\theta_{16}$ , and plot of smoothed transmission factors,  $\psi_{16}$ , for FLOWS station No. 23, located on the west runway at the Memphis International Airport. The correlation between the obstruction angles and the transmission factors is  $-0.91$ .

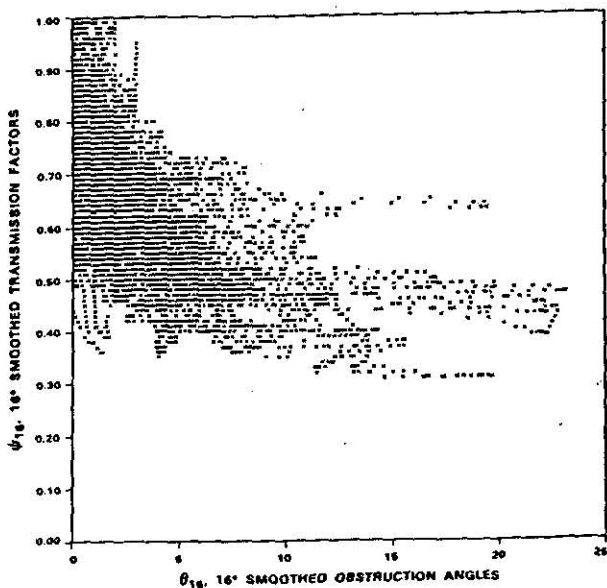


Figure 3. Plot of smoothed transmission factors ( $\psi_{16}$ ) versus smoothed obstruction angles ( $\theta_{16}$ , in degrees), for all stations for all azimuths.

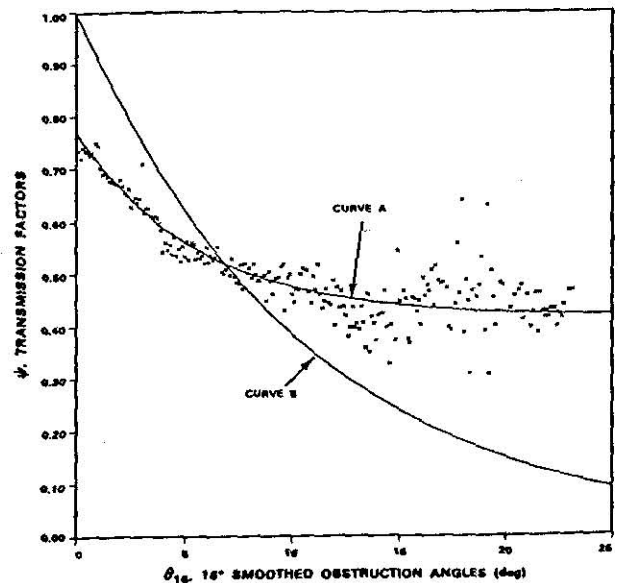


Figure 4. Plot of the mean of all the smoothed transmission factors ( $\psi_{16}$ ) for each  $0.1^\circ$  step in obstruction angle ( $\theta_{16}$ ). The best fit exponential curve (curve A, given by Eq. (8)) is plotted through these points. The other curve (curve B) is the exponential fit used by Fujita and Wakimoto (1982):  $\psi = \exp[-0.0948 \theta]$ .